

Flexible nanovectors

Nicola M Pugno

Department of Structural Engineering, Politecnico di Torino, Corso Duca degli Abruzzi 24,
10129 Torino, Italy
and
National Institute of Nuclear Physics, National Laboratories of Frascati, Via E Fermi 40,
00044 Frascati, Italy

E-mail: nicola.pugno@polito.it

Received 23 April 2008, in final form 23 July 2008

Published 6 November 2008

Online at stacks.iop.org/JPhysCM/20/474205

Abstract

In this paper we show that the control of adhesion in highly flexible (a property that could be crucial for smart drug delivery but which is still ignored in the literature) nanovectors can help in smartly targeting and delivering the drug. The existence of and the conditions for activating and controlling a super-adhesive state are addressed. Even if such a state has never been observed in nanovectors, our calculations, as well as observations in spiders and geckos, suggest its existence and feasible control. Control of the competition between the drag and the adhesive force is exploited to improve the targeting ability and a hierarchical model is applied to describe a real vasculature. The high flexibility of the nanovector is used to smartly deliver the drug only during adhesion by nanopumping or, as a limiting case, by the new concept of 'adhesion induced nanovector implosion'; a liquid drop analogy is utilized for the calculations. Fast (pumping) and slow (diffusion) drug deliveries can thus be separately controlled by controlling the size and shape of the nanovector. Multiple stage nanovectors are also briefly discussed, mimicking aerospace vector strategies.

(Some figures in this article are in colour only in the electronic version)

1. Introduction

Injectable drug delivery nanovectors (including nanocarriers, nanoparticles, nanoshells, etc) are used in nanomedicine for cancer therapy, specifically for multiple drug delivery, thermal ablation or imaging (see the recent reviews [1, 2]). These vectors must be large enough to evade the body's defences but sufficiently small to avoid blockages of the capillaries, and thus are nanosized by definition.

Nanovectors can extravasate into the tumour through the enhanced permeation and retention (EPR) effect [3], roughly schematized in figure 1. The increased permeability of the blood vessels, i.e. the formation of new vessels from existing ones, leads to the permeation of nanovectors into the tumour; moreover, its dysfunctional lymphatic drainage retains them, allowing localized drug delivery. Experiments with liposomes suggest that extravasation into tumours can take place if the liposome diameter is <400 nm [4] and becomes more effective for sizes <200 nm [4–7]. Unfortunately some tumours do not exhibit the EPR effect, and this passive strategy could also induce a lack of control and thus multiple drug resistance [2].

To overcome these limitations nanovectors are functionalized in order to actively bind to specific cells after extravasation, through ligand–receptor interactions. To maximize specificity, a surface marker (receptor or antibody) should be overexpressed on target cells relative to normal ones. It is generally accepted that higher binding affinity increases targeting efficacy. However, for solid tumours, this could reduce penetration due to a binding-site barrier, where the nanovectors binds to its target so strongly that penetration into the tissue is prevented [8, 9]. This suggests the importance of optimizing adhesion in nanovectors, which is the aim of the present paper. Moreover, cancer cells often overexpress the receptors for nutrition, thus interaction of growth factors or vitamins with cancer cells is an additional commonly used targeting strategy.

Finally, the nanovectors are activated and release their cytotoxic effect when irradiated by external energy or induced by environmental conditions such as metabolic markers or the acidity levels that accompany inflammatory states, infections and neoplastic processes [1].

Nanosized vectors include fusion proteins and immunotoxins/polymers (3–15 nm), dendrimers (~ 5 nm), polymer–

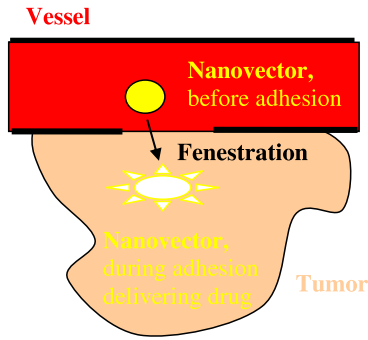


Figure 1. A simplified scheme describing the concept of nanovector therapeutics.

drug conjugates (6–15 nm), micelles (5–100 nm, lipid-based or polymeric), nanoparticles (10–40 nm, gold, for photothermal ablation; 50–200 nm, polymeric), liposomes (85–100 nm), polymersomes (~100 nm), immunoliposomes (100–150) and nanoshells (gold–silica, ~130 nm, photothermal therapy) [2]. Absorbing nanoshells are suitable for hyperthermia-based therapeutics: they absorb radiation and heat up the surrounding cancer cells. Above a thermal threshold irreversible damage selectively kills the cancer cells [2]. To achieve temporal release of two drugs, composite polymer core/lipid shell structures can be adopted [10].

Polymers are the most commonly explored materials for nanovectors. Lipid-based nanovectors have attractive biological properties, such as biocompatibility, biodegradability (not required for sizes <5 nm) and isolation of drugs from the surrounding environment. Between them the most famous are liposomes, single- or multi-bilayered (within inner aqueous phases) spherical particles. They have shown preferential accumulation in tumours via the EPR effect. However, liposomes that circulate for too long may lead to extravasation of the drug into undesired sites. A long circulating half-life, soluble or colloidal behaviour, high binding affinity, biocompatibility, easy functionalization, easy intracellular penetration, controlled pharmacokinetics and high drug protection are all characteristics simultaneously required for optimal nanocarrier design.

However, controlling, under the body’s defences, both targeting and drug delivery remains a complex task. Mechanical studies can have a role in this, as suggested by the adhesion of colloids on a cell surface in competition for mobile receptors [11] or in receptor-mediated endocytosis [12]. In this paper we will introduce the new concept of smart, highly flexible (a property that could be crucial for smart drug delivery but which is still ignored in the literature) nanovectors, based on smart adhesion [13, 14]. Adhesion between a nanovector and a cellular substrate is governed by the adhesion energy (van der Waals, electrostatic, steric, etc) per unit area and, due to the tremendous surface to volume ratio of nano-objects, becomes predominant at the nanoscale. Geckos and spiders take advantage of this [14], and nanovectors could do the same. The existence and the conditions for activating and controlling a super-adhesive state, as done by spiders and geckos [14], are addressed in this paper for nanovectors.

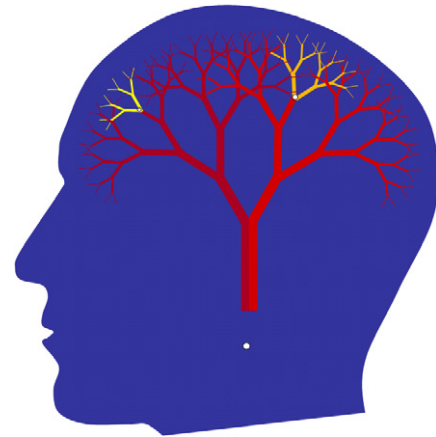


Figure 2. A fractal model to describe the real hierarchical vasculature and a nanovector reaching the desired site. Reproduced with permission courtesy of Emma Chung [15].

During adhesion the smart nanovector considerably changes its shape in a controllable way and, sometimes, can implode due to buckling [16]. Thus, the high flexibility of the nanovector is used to release the drug only during adhesion, by a nanopumping mechanism; a liquid drop analogy [13] is used for the calculations. Fast (pumping) and slow (diffusion) drug delivery can thus be separately controlled. Such a mechanism smartly delivers the drug in a controllable way, ideally aborting tumour colonization [17]. Multiple stage nanovectors are also considered, envisioning molecular motors too, mimicking the well-established strategies of aerospace vectors.

2. The hierarchical vasculature: a fractal model

A fractal model can describe the real hierarchical vasculature [18], see figure 2.

For humans, a vessel of diameter d_j typically branches into $n = 3$ sub-vessels [19, 20], of diameters d_{j+1} , with a law of the type $d_j^k = n d_{j+1}^k$. For area-preserving branching $k = 2$, even if also $k = 3$ is used; in general $2 \leq k \leq 3$ [21–23]. This law is a consequence of an assumed relation between vessel diameter d_j and flow rate q_j in the form $q_j \propto d_j^k$. We here assume the classical value $k = 2$, even if towards the capillaries $k = 3$ could perhaps better describe the observations [18, 24]. The number of vessels at the hierarchical level j is

$$N_j = n^j \tag{1}$$

thus that of capillaries is $N_C = n^N$, where N is the number of hierarchical levels. Each capillary serves a volume $V_C \approx V_{\text{human}}/N_C$, where V_{human} is the characteristic volume of a man (of the order of 0.1 m³). Plausibly considering $N_C = V_{\text{human}}/V_C \approx 10^{10}$ [18], we expect $N \approx 21$. From $d_j^k = n d_{j+1}^k$ we can calculate the size of the vessel at the level j as

$$d_j/d_0 = n^{-j/k} \tag{2}$$

thus $d_C/d_0 = n^{-N/k}$ where $d_C \equiv d_N$ is the capillary diameter. Taking $k = 2$, $N = 21$, $n = 3$ yields $d_0/d_C \approx 10^4$; considering $d_0 \approx 3$ cm as the size of the aorta gives $d_C \approx 3 \mu\text{m}$, plausible for a capillary [18, 25–28]. The velocities v_j in the vessels can be calculated noting that $q_j \propto N_j v_j d_j^k = \text{const}$, thus

$$v_j/v_0 = n^{j/k-j}. \quad (3)$$

Accordingly, $v_0/v_C = n^{N-N/k}$ is the ratio between the velocities in the aorta and in the capillaries. Taking $k = 2$, $N = 21$ and $n = 3$ we have $v_0/v_C \approx 10^5$, suggesting a very slow flow in the capillaries.

Statistically, a drug D1 contained in a nanovector is delivered to the desired capillary with a probability N_C^{-1} . Thus, to release at the same site all the needed drugs D1, . . . , D*l*, at the same site the probability decreases drastically up to N_C^{-l} . However, introducing *l* drugs in the same nanovector would increase the probability again up to N_C^{-1} . Multifunctional nanovectors are thus required. Roughly speaking, a large number of capillaries serve the same physical site (see, e.g., figure 2), so that the probability of reaching the target becomes N_S^{-1} , where $N_S = V_{\text{human}}/V_S \approx 10^5$ is the number of sites, each of them plausibly defined by a volume $V_S \approx 1 \text{ cm}^3$. The EPR effect, ligand–receptor interactions and long circulating half-life enhance the probability of reaching the target, which, due to the body defences, remains of the order of 10^{-4} . In spite of this, their to their miniaturized size, a large number (the volume occupied by a red blood cell could host 1 million nanoparticles of diameter 10 nm) of nanovectors can participate at the competition and thus some of them will probably reach the target.

We may observe that tumours too are hierarchical in nature [29–32], suggesting the importance of a fractal approach in this context.

3. Adhesion of largely deformed nanovectors: a liquid drop analogy

The adhesion of liquid drops is a fascinating field, 200 years old (see the notable review by Quèrè [33]), and could present analogies with the adhesion of nanovectors [34], e.g. as recently observed for nanotubes [13]. For highly flexible nanovectors the inevitable presence of large displacements, deformations and contacts renders the problem out of the domain of linear elasticity and into that of the elastic theory of shells, for which only numerical integrations can be obtained, e.g. [16]. A liquid drop analogy could help in solving the problem, even if only in an approximate way: accordingly, we are going to extend the approach developed for cylindrical symmetry in [13] (applied to nanotubes) to spherical symmetry (for nanovectors).

The adhesion of a (small, for which surface tension prevails on gravity) liquid drop is fully described by the contact angle θ (a function of the liquid/solid/vapour surface energies) between drop and substrate (see figure 3(a)). Indicating with R_0 the radius of the drop in air and with R the radius of curvature of the spherical cap describing the adhering drop, the radius of the contact area a can be calculated using mass

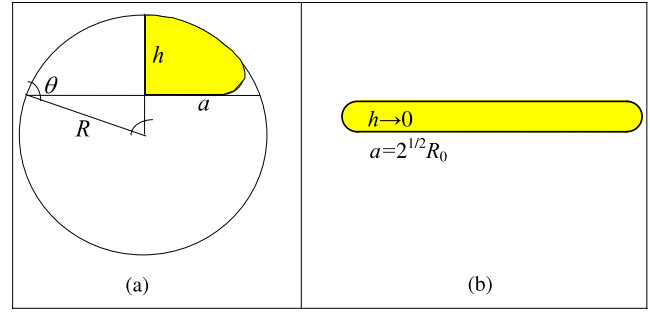


Figure 3. Nanovector (liquid drop) geometry, under large contact/deformation (a) and squashed configuration (b).

conservation. The adhesion of a nanovector of radius R_0 can be similarly described by an equivalent contact angle θ (that we expect to be a function of the adhesion work and bending stiffness), the radius of curvature R of the deformed non-contact cap and the contact radius $a = R \sin \theta$; thus the (maximum) height of the deformed nanovector is $h = R(1 - \cos \theta)$ (see figure 3(a)). Assuming a porous membrane of the nanovector, thus capable of exchanging mass and delivering the drug, surface inextensibility rather than mass conservation has to be imposed, i.e. $S = 2\pi Rh + \pi a^2 = 4\pi R_0^2$ (figure 3(a)). Accordingly we deduce:

$$\frac{a}{R_0} = \frac{2}{\sqrt{1 + 2(1 - \cos \theta)/\sin^2 \theta}}. \quad (4)$$

For small contacts $\theta \rightarrow \pi$ and $a/R_0 \approx \sqrt{2 \sin^2 \theta / (1 - \cos \theta)}$. This asymptotic solution can be directly compared with the analytical result posed by elasticity for a spherical shell with Young’s modulus E , Poisson’s ratio ν , thickness t and contact surface energy γ , which yields $a/R_0 \approx \sqrt{2\sqrt{12}\pi R_0 \gamma / \{E t^2\}}$ [35]; thus, we can define the contact angle for a nanoshell (e.g. liposome) according to

$$\begin{cases} \frac{\sin^2 \theta}{1 - \cos \theta} = \frac{R_0}{R_0^*} & R_0 \leq 2R_0^* \\ \frac{\sin^2 \theta}{1 - \cos \theta} = 2 & R_0 > 2R_0^* \end{cases} \quad (5)$$

$$R_0^* = \frac{E t^2}{\pi \sqrt{12} \gamma (1 - \alpha)},$$

in which the parameter $0 \leq \alpha \leq 1$ takes into account the stiffening caused by the presence of a material (e.g. particles, liquid-like, etc) inside the nanovector. For a porous membrane $\alpha \approx 0$ and the mass exchange has a vanishing energy cost. We have found that for a compact nanosphere equation (5) would remain valid with $R_0^* = 2R_0 \{2ER_0 / (3\pi\gamma)\}^{2/3}$.

According to equation (5), the contact will be hydrophobic or, better, nanovector-phobic ($\theta > \pi/2$, water/nanovector repellent) or nanovector-philic ($\theta < \pi/2$) for $R_0 < R_0^*$ or $R_0 > R_0^*$; or even super-nanovector-phobic/philic ($\theta \approx \pi$, 0) for $R_0 \rightarrow 0$ or $R_0 \geq R_0^{(C)} = 2R_0^*$. For example, for a fullerene $E \approx 1 \text{ TPa}$, $t \approx 0.34 \text{ nm}$, $\gamma \approx 0.2 \text{ J m}^{-2}$ (C–C van der Waals), $R_0^* \approx 53 \text{ nm}$, i.e. beyond a $C_{1000000}$ molecule. Super-nanovector-phobic behaviour results in a high

motility, whereas super-nanovector-philic behaviour is ideal for maximizing adhesion. Note that equation (5) implies that the contact area becomes maximal ($\theta = 0$) for $R_0 \geq R_0^{(C)} = 2R_0^*$ and thus not only for $R_0 \rightarrow \infty$. This corresponds to a kind of implosion [16] (figure 3(b)).

Introducing equation (5) into equation (4) we find the following nonlinear law:

$$\begin{aligned} \frac{a}{R_0} &= \frac{2}{\sqrt{1 + 2R_0^*/R_0}} & R_0 \leq 2R_0^* \\ \frac{a}{R_0} &= \sqrt{2} & R_0 > 2R_0^*. \end{aligned} \quad (6)$$

For small contacts/deformations ($\theta \rightarrow \pi$) the prediction of equation (6) is identical to the asymptotic solution reported in [35], whereas for large contacts/deformations ($\theta \rightarrow 0$) $a/R_0 = \sqrt{2}$, as coherently imposed by the condition of inextensible (figure 3(b)).

The (maximum) height of the flattened nanovector and its radius of curvature can be geometrically derived as (figure 3(a)):

$$\frac{h}{a} = \frac{1 - \cos \theta}{\sin \theta}, \quad \frac{R}{a} = \frac{1}{\sin \theta}. \quad (7)$$

For $\theta \rightarrow 0$, $h/a \rightarrow 0$ and $R/a \rightarrow \infty$, whereas for $\theta \rightarrow \pi$, $h/(2R_0) \rightarrow 1$ and $R/R_0 \rightarrow 1$, confirming that the theory is self-consistent.

4. Nanovector elastic energy and delamination: the super-adhesive state

During the loss of adhesion, i.e. delamination, the classical fracture mechanics energy balance must hold. Accordingly, the opposite of the variation of the total potential energy (elastic energy minus external work) with respect to the crack surface area (complementary to the contact area) must be equal to the work of adhesion 2γ (see [36, 37] for a quantized approach). Thus $d\Phi = 2\gamma d(\pi a^2)$ (the external work here is zero), where Φ denotes the elastic energy stored in the nanovector. By integration, following [13, 38, 39], we can calculate the energy stored in the largely deformed nanovector simply as

$$\Phi = 2\gamma\pi a^2. \quad (8)$$

In order to calculate the force for delaminating the nanovector we have to include the external work W in the energy balance, which consequently becomes $d\Phi - dW = 2\gamma d(\pi a^2)$, where $dW \approx -Fda$ (F is assumed to be applied at the nanovector centroid). The stored elastic energy is related to the external work via $d\Phi = \beta dW$, in which $0 \leq \beta \leq 1$ takes into account the system nonlinearity: $\beta = 1/2$ for linear systems, as imposed by the Clapeyron theorem; $\beta = 0$ for rigid systems, whereas $\beta = 1$ corresponds to the other (opposite) limiting case (as can be evinced by the next equation). Consequently, the force needed for delaminating the nanovector, or the adhesion force, is

$$F_A = \frac{4\pi}{1 - \beta} \gamma a. \quad (9)$$

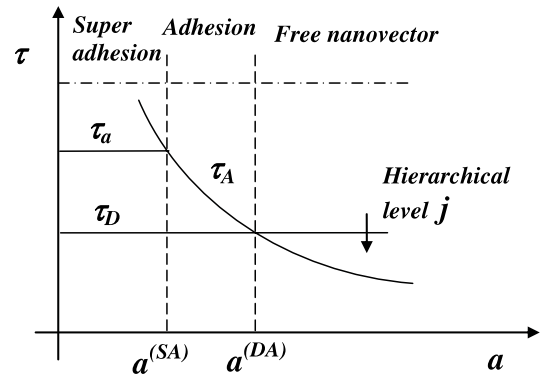


Figure 4. Nanovector adhesive map design. The super-adhesive state and the competition between drag and adhesive forces ($a^{(DA)} \equiv A/\ell^{(DA)}$).

The important consequence of equation (9) is that $F_A \propto a$ and not to a^2 , thus the adhesive failure shear stress, τ_A , is size-dependent:

$$\tau_A = \frac{F_A}{\pi a^2} = \frac{4}{1 - \beta} \frac{\gamma}{a}. \quad (10)$$

Equation (10) shows that nanovectors with smaller contact sizes a will have higher failure stresses. Obviously τ_A cannot tend to infinity, being ultimately limited by the intrinsic adhesion shear strength τ_a . Accordingly, the nanovector will have a phase transformation entering in a ‘super-adhesive state’ for $a < a^{(SA)}$, where

$$a^{(SA)} = \frac{4}{1 - \beta} \frac{\gamma}{\tau_a} \quad (11)$$

corresponding to a super-adhesive failure stress $\tau_A^{(SA)} = \tau_a$ and force $F_A^{(SA)} = \tau_a \pi a^2$ (see figure 4). Thus a nanovector with size smaller than $R_0^{(SA)} = a^{(SA)}/\sqrt{2}$ is by definition super-adhesive.

The peculiarity of having a high motility is fundamental for a nanovector to reach the target. We could also design nanovectors to have a phase transformation into the super-adhesive state only when the desired site is reached. The nanosized dimensions of the spatulas of geckos and spiders make it possible for them to walk in the super-adhesive state, in which the ability to controlling adhesion becomes even more crucial and fundamental.

5. Competition between drag and adhesive forces: controlling adhesion

The drag force acting on the nanovector is proportional to its cross-sectional area A exposed to the blood flow. It can be calculated according to geometrical considerations (see figure 3(a)) as

$$\begin{aligned} A &= \theta R^2 - a(R - h) = f(\theta) h^2, \\ f(\theta) &= \frac{\theta - \sin \theta + (1 - \cos \theta) \sin \theta}{(1 - \cos \theta)^2}. \end{aligned} \quad (12)$$

(We have chosen to formally put A as proportional to h^2 , instead of ah or a^2 , since A does not tend to zero for vanishing a .)

The drag force can be written as $F_D = \rho C_D A v^2 / 2$, where ρ is the density of the blood, v is the relative velocity of the nanovector (with respect to the blood flow, having velocity v_j) and C_D is the drag coefficient. For turbulent flow (i.e. Reynolds numbers $Re > 1000$ where $Re = R_0 \rho v / \eta$ and η is the blood dynamic viscosity) the drag coefficient is approximately constant, whereas for laminar flow ($Re < 1$) becomes inversely proportional to the velocity, so that $F_D \propto v$. Accordingly we could write

$$F_D = \frac{1}{2} \rho C_x A v^x, \quad x = 1 - 2 \quad (13)$$

where C_x is a ‘generalized’ drag coefficient (with different physical units for different values of x). Thus, a drag shear stress can be defined as

$$\tau_D = \frac{F_D}{\pi a^2} = \frac{\rho C_x A v^x}{2\pi a^2}. \quad (14)$$

In the blood flow both turbulent (and pulsatile, near the heart), transitional and laminar (and non-pulsatile, towards the capillaries) flows are present; the turbulence tends to vanish at a hierarchical level $j \approx 7$ [18]. In order to avoid the premature adhesion of the nanovector $F_D > F_A$, whereas only at the desired site we want $F_D = F_A$. Equating equations (9) and (13) gives a critical length

$$\ell^{(DA)} = \frac{8\pi\gamma}{(1 - \beta) \rho C_x v^x}. \quad (15)$$

Defining $\ell = A/a$, for $\ell < \ell^{(DA)}$ the adhesion force prevails, whereas for $\ell > \ell^{(DA)}$ the drag force prevails. If the desired site is in the capillaries, then $x = 1$ (laminar flow).

Summarizing, for $\ell < \ell^{(DA)}$ and $a < a^{(SA)}$ adhesion takes place in the super-adhesive state, or for $\ell < \ell^{(DA)}$ and $a > a^{(SA)}$ out of it; for $\ell > \ell^{(DA)}$ adhesion does not occur (see figure 4).

6. Controlling the drug delivery: nanopump nanovectors

Drug delivery should take place at the desired site, where the nanovector must adhere. Designing a nanovector of size R_0 with a proper elasticity, or R_0^* (see equation (5)), allows us to control the volume variation of the nanovector induced by the adhesion energy (see figure 5). If the nanovector membrane is perfectly porous ($\alpha \approx 0$) an equivalent volume ΔV_{fast} of drug (we assume here an ideal nanopump, thus a unitary efficiency) will be smartly and suddenly delivered only at the target. The nanovector works here as a nanopump. Geometrically we find

$$\Delta V_{\text{fast}} = \frac{4}{3} \pi R_0^3 - \frac{\pi}{3} (2 + \cos \theta) (1 - \cos \theta)^2 R^3. \quad (16)$$

As a limiting case for $R_0 = 2R_0^*$, i.e. $\theta = 0$, $\Delta V_{\text{fast}} = 4\pi R_0^3/3$. Diffusive slow mechanisms will release

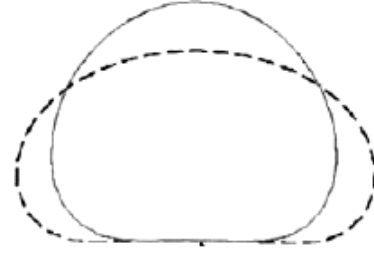


Figure 5. Adhesion-induced nanopumping.

the remaining amount of drug, still contained in the deformed nanovector after adhesion, that is:

$$\Delta V_{\text{slow}} = \frac{\pi}{3} (2 + \cos \theta) (1 - \cos \theta)^2 R^3. \quad (17)$$

We could thus control separately fast and slow drug deliveries in order to optimize drug efficiency by realizing a two-stage temporal nanovector. As a limiting case, adhesion induced implosion of the nanovector can be required.

The nanopumping mechanism will be activated in addition to different delivery strategies, e.g. endocytosis, and could be used for a global optimal design. For example, endocytosis is predicted with a maximal efficiency for particles having size R ($2/R = 1/R_{p1} + 1/R_{p2}$ for non-spherical geometry, in which $1/R_{p1,2}$ are the Gaussian principal curvatures) of ~ 20 – 30 nm, with characteristic wrapping times of ~ 1 – 60 s [12]. Thus the drug efflux (slow or fast) can be engineered to occur upon adhesion to the cell membrane, or rather inside the cell. An optimal colloid concentration also emerges [11]. We could imagine delivery by nanopumping sub-nanocarriers with optimal size for endocytosis, once the target has been reached, producing a smart multiple stage nanovector.

7. Multiple stage nanovectors: mimicking aerospace vector strategies

Multiple stage nanovectors [10, 40] could also be designed, formally considering the first target as the place corresponding to the activation of the second stage and the drug particles as sub-nanovectors, and so on for multiple stages. The nanovector can be optimized for a specific stage, as with aerospace vectors. Molecular motors could also be envisioned [1].

A multiple stage nanovector could be designed to eject its sub-nanovectors and adhere in the vessel/site having a ‘signature’ described by the following blood velocity:

$$v_j = \sqrt[x]{\frac{8\pi\gamma}{(1 - \beta) \rho C_x \ell^{(DA)}}}. \quad (18)$$

If R_1 is the radius of the sub-nanovectors, a number

$$M_{\text{slow}}^{\text{fast}} \approx \phi \Delta V_{\text{slow}}^{\text{fast}} / (4\pi R_1^3/3) \quad (19)$$

of them will be rapidly/slowly ejected, where $\phi \approx 1$ is the packing factor. Multiple stages can thus be designed by controlling adhesion, repeating the outlined process. Note that,

from equation (9), the ratio between the total adhesion forces required to delaminate the M sub-nanovectors and the mother nanovector is $F_A^{(M)} = M^{2/3} F_A$, and for m stages:

$$F_A^{(M_m, m)} = M_m^{2m/3} F_A \quad (20)$$

where M_m is the number of sub-nanovectors at the stage m . Increasing the adhesive ability of the system by increasing the number of hierarchical levels, imposed by the scaling of the adhesive failure shear stress, is evident. Obviously this gain cannot continue *ad infinitum* and the force will be limited by the intrinsic adhesive strength, which is maximal in the super-adhesive state. Spiders and geckos use the same strategy: the (volumetric) coefficient $2/3$ in equation (20) is replaced by the (superficial) factor of $1/2$, showing that dividing a contact into 100 subcontacts leads to an increase in the adhesion strength by one order of magnitude. Geckos use billions of contacts for such a purpose [14].

8. Conclusions

In this paper we have shown that controlling super-adhesion in highly flexible nanovectors can help in smartly targeting and delivering a drug. The existence of and the conditions for activating and controlling the super-adhesive state have been demonstrated and elucidated. Even if a super-adhesive state has never been observed in nanovectors, our theoretical considerations as well as observations of geckos and spiders suggest its existence and feasible control. Amazing new therapeutic strategies are thus expected by controlling the super-adhesive state in nanovectors and their flexibility, via advanced nanomechanical calculations [41]. We have also shown that the control of the competition between the drag and the adhesive forces could be used to improve the targeting ability within a hierarchical vasculature. The physicochemical characteristics of the drug itself, rather than of the carrier, are not expected to have a major affect on the nanovector adhesion but could significantly affect the induced release: additional analyses are thus required. The high flexibility of the nanovector is used to release the drug only during adhesion by nanopumping and, as a limiting case, by the new concept of ‘adhesion induced nanovector implosion’; a liquid drop analogy has been used for the calculations even though numerically exact solutions are still under study. Fast (pumping) and slow (diffusion) drug deliveries can thus be separately controlled. Multiple spatial-temporal stage nanovectors have been also discussed, mimicking aerospace vector strategies, e.g. for optimal endocytosis.

Acknowledgments

The author is supported by the ‘Bando Ricerca Scientifica Piemonte 2006’–BIADS: Novel biomaterials for intraoperative adjustable devices for fine tuning of prostheses shape and performance in surgery.

References

- [1] Ferrari M 2005 Cancer nanotechnology: opportunities and challenges *Nat. Rev. Cancer* **5** 161–71

- [2] Peer D, Karp J M, Hong S, Farokhzad O C, Margalit R and Langer R 2007 Nanocarriers as an emerging platform for cancer therapy *Nat. Nanotechnol.* **2** 751–60
- [3] Matsumura Y and Maeda H 1986 A new concept for macromolecular therapeutics in cancer-chemotherapy. Mechanism of tumorotropic accumulation of proteins and the antitumor agent smancs *Cancer Res.* **46** 6387–92
- [4] Yuan F 1995 Vascular-permeability in a human tumor xenograft. Molecular-size dependence and cutoff size *Cancer Res.* **55** 3752–6
- [5] Torchilin V P 2005 Recent advances with liposomes as pharmaceutical carriers *Nat. Rev. Drug Discov.* **4** 145–60
- [6] Hobbs S K *et al* 1998 Regulation of transport pathways in tumor vessels: role of tumor type and microenvironment *Proc. Natl Acad. Sci. USA* **95** 4607–12
- [7] Couvreur P and Vauthier C 2006 Nanotechnology: intelligent design to treat complex disease *Pharm. Res.* **23** 1417–50
- [8] Allen T M 2002 Ligand-targeted therapeutics in anticancer therapy *Nat. Rev. Cancer* **2** 750–63
- [9] Adams G P *et al* 2001 High affinity restricts the localization and tumor penetration of single-chain Fv antibody molecules *Cancer Res.* **61** 4750–5
- [10] Sengupta S *et al* 2005 Temporal targeting of tumour cells and neovasculature with a nanoscale delivery system *Nature* **436** 568–72
- [11] van Effenterre D and Roux D 2003 Adhesion of colloids on a cell surface in competition for mobile receptors *Europhys. Lett.* **64** 543–9
- [12] Gao H, Shi W and Freund L B 2005 Mechanics of receptor-mediated endocytosis *Proc. Natl Acad. Sci. USA* **102** 9469–74
- [13] Pugno N 2008 An analogy between the adhesion of liquid drops and single-walled nanotubes *Scr. Mater.* **58** 73–5
- [14] Pugno N 2007 Towards a Spiderman suit: large invisible cables and self-cleaning releasable super-adhesive materials *J. Phys.: Condens. Matter* **19** 395001
- [15] Chung E 2007 *Embolism and Cerebral Ischemia in a Fractal Vascular Tree* http://www.le.ac.uk/cv/research/Ultrasound/Emma/Emma_research.html
- [16] Tamura K, Komura S and Kato T 2004 Adhesion induced buckling of spherical shells *J. Phys.: Condens. Matter* **16** L421–8
- [17] Guiot C, Pugno N and Delsanto P P 2006 An elastomechanical model for tumor invasion *Appl. Phys. Lett.* **89** 233901
- [18] West G B, Brown J H and Enquist B J 1997 A general model for the origin of allometric scaling laws in Biology *Science* **276** 122–6
- [19] Caro C G *et al* 1978 *The Mechanics of Circulation* (Oxford: Oxford University Press)
- [20] Fung Y C 1984 *Biodynamics: Circulation* (New York: Springer)
- [21] Roy A G and Woldenberg M J 1982 A generalization of the optimal models of arterial branching *Bull. Math. Biol.* **44** 349–60
- [22] Sherman T F 1981 On connecting large vessels to small. The meaning of Murray’s Law *J. Gen. Physiol.* **78** 431–53
- [23] Woldenberg M J and Horsfield K 1983 Finding the optimal length for three branches at a junction *J. Theor. Biol.* **104** 301–18
- [24] Zamir M P, Sinclair P and Wonnacott T H 1992 Relation between diameter and flow in major branches of the arch of the aorta *J. Biomech.* **25** 1303–10
- [25] Calder W A 1978 *Size, Function and Life History* (Cambridge, MA: Harvard University Press)
- [26] McMahon T A and Bonner J T 1983 *On Size and Life* (New York: Scientific American Library)
- [27] Peters R H 1983 *The Ecological Implications of Body Size* (Cambridge, MA: Cambridge University Press)
- [28] Schmidt-Nielsen K 1984 *Scaling; Why is Animal Size So Important?* (Cambridge, MA: Cambridge University Press)

- [29] Guiot C, Delsanto P P, Carpinteri A, Pugno N, Mansury Y and Deisboeck T S 2006 The dynamic evolution of the power exponent in a universal growth model of tumors *J. Theor. Biol.* **240** 459–63
- [30] Guiot C, Pugno N, Delsanto P P and Deisboeck T S 2008 Physical aspects of cancer invasion *Phys. Biol.* **5** P1–6
- [31] Deisboeck T S, Guiot C, Delsanto P P and Pugno N 2006 Does cancer growth depend on surface extension? *Med. Hypotheses* **67** 1338–41
- [32] Pugno N 2007 A statistical analogy between collapse of solids and death of living organisms: proposal for a ‘Law of Life’ *Med. Hypotheses* **69** 441–7
- [33] Querè D 2005 Non-sticking drops *Rep. Prog. Phys.* **68** 2495–532
- [34] Decuzzi P and Ferrari M 2006 The adhesive strength of non-spherical particles mediated by specific interactions *Biomaterials* **27** 5307–14
- [35] Elsner N, Dubreuil F and Fery A 2004 Tuning of microcapsule adhesion by varying the capsule-wall thickness *Phys. Rev. E* **69** 031802
- [36] Pugno N M and Ruoff R 2004 Quantized fracture mechanics *Phil. Mag.* **84** 2829–45
- [37] Pugno N 2006 Dynamic quantized fracture mechanics *Int. J. Fract.* **140** 159–68
- [38] Tang T, Jagota A and Hui C-Y 2005 Adhesion between single-walled carbon nanotubes *J. Appl. Phys.* **97** 074394
- [39] Glassmaker N J, Jagota A, Hui C-Y and Kim J 2004 Design of biomimetic fibrillar interfaces: 1. Making contact *J. R. Soc. Interface* **1** 23–33
- [40] Sakamoto J, Annapragada A, Decuzzi P and Ferrari M 2007 Antibiological barrier nanovector technology for cancer applications *Expert Opin Drug Deliv.* **4** 359–69
- [41] Pugno N M 2007 *The Nanomechanics in Italy Research Sign Post* (Kerala: Research Signpost)